Available online at www.elixirpublishers.com (Elixir International Journal)

Magnetic Materials

Elixir Magnetic Materials 61 (2013) 16757-16760

ISSN: 2229-712X

Structural, electrical and magnetic study of $La_{0.5}Ca_{0.5}MnO_3$ ceramics

Khalid Sultan[1,*], M. Ikram[1] and K.Asokan[2]

[1]Department of Physics, National Institute of Technology Hazratbal Srinagar, J & K-190006, India

[2]Material Science Division, Inter University Accelerator Centre, Aruna Asaf Ali Marg, New Delhi-110067, India

ARTICLE INFO

Article history:

Received: 3 July 2013;

Received in revised form:

24 July 2013;

Accepted: 1 August 2013;

Keywords

Solid State Reaction,

Divalent doping,

Magnetization,

Zener double exchange.

ABSTRACT

Polycrystalline bulk samples of $La_{0.5}Ca_{0.5}MnO_3$ were synthesized by solid state reaction method to explore their structural, electrical and magnetic properties. The Rietveld treatment of the X-Ray diffraction (XRD) profiles clearly indicated that the XRD patterns are well fitted with Orthorhombic structure. Raman peaks revealed their finger print positions and irreducible representations at the Brillouin zone center as presented by the group theory. Resistivity 'ρ' measurements revealed that ρ first increases as temperature 'T' decreases, exhibits a peak at T = Tp (Tp is the temperature corresponding to the resistivity peak), which is around 150 K in the present compound and then decreases as *T* is further reduced below *Tc (*Tc is the ferromagnetic curie temperature). For *T* > *Tc*, the resistivity shows activated transport as in an insulator. Magnetization study revealed that both a paramagnetic to ferromagnetic transition and an antiferromagnetic transition are involved. Possible mechanism contributing to these processes such as activated transport and Zener double exchange has been discussed.

© 2013 Elixir All rights reserved

1.Introduction

The fascinating physical phenomena in manganites are dominated by the competition of two prominent ground states, namely ferromagnetic metallic and charge-ordered insulating phases. Mixed valent manganites are noted for their unusual magnetic, electronic and structural phase transitions. The effect of divalent doping in transition metal oxides was studied intensely since the discovery of Colossal magnetoresistance (CMR) [1] and has been interest of recent study also [2]. The rich phase diagram of $La_{1-x}R_xMnO_3$ where 'R' is a divalent ion (e.g., Sr, Ca) is a result of interplay between spin, charge, lattice and orbital degrees of freedom [3]. The partial substitution of trivalent La by divalent Ca results in hole doping. In the parent compound of $LaMnO_3$, "La" is partially substituted by divalent cations such as Ca, Sr etc to achieve a high CMR. The parent compound, $LaMnO_3$ (Mn^{3+}; t_{2g} 3, e_g 1) is an antiferromagnetic insulator. Divalent substitution for La^{3+}, in the simplest picture, converts Mn^{3+} ions to Mn^{4+}. The latter is not Jahn-Teller active, thus the average MnO_6 distortion decreases with increasing x. The range of this substitution of Ca, Sr or even Ce is limited by the tolerance factor 't' [which is defined as the ratio of the distance between the cation and the oxygen ions and the Mn-O bond length divided by √2].

i,e $t = d_{R-O}/\sqrt{2}\, d_{Mn-O}$

Only for the Ca doped $LaMnO_3$ the tolerance factor is close to one and the alloy $La_{1-x}Ca_xMnO_3$ (LCMO)can form over the entire concentration range, $0 \leq x \leq 1$ [4].

In the compound LCMO, the Mn ions form approximately a cubic lattice with the oxygen ion located nearly at the center of each side and the La or Ca atoms at the body center of each cube. In the nearly cubic symmetry, the five degenerate 3d levels split into t_{2g} (triplet) and e_g (doublet). In the octahedral coordination, e_g states have higher energy than the corresponding t_{2g} states. The hole doped system LCMO is a mixture of trivalent Mn^{3+} and tetravalent Mn^{4+} ions. With this mixed valency of Mn ions in the system, all the t_{2g} orbitals in both trivalent and tetravalent Mn are singly occupied and results in a total spin of 3/2 in the system. The situation is different for the e_g orbitals, in Mn^{4+} ($3d^3$) the e_g orbitals are empty while as in Mn^{3+} ($3d^4$) e_g orbitals are occupied by a single 3d electron. The t_{2g} and e_g orbitals are ferromagnetically correlated via Hund's rule. The intermediate valence character of Mn ions arises from the hoping of e_g electrons [5-6].

The parent compound $LaMnO_3$ is an antiferromagnetic insulator and the divalent doping at La sites results in the phenomena of CMR in the compound $La_{1-x}R_xMnO_3$ for the doping range of $0.2 < x < 0.5$ [7]. These compounds show a paramagnetic-to-ferromagnetic phase transition accompanied by a sharp drop in resistivity of the compounds. The phenomena of CMR occur in these materials as a consequence of rapid shift of ferromagnetic transition temperature (Tc) to higher temperature region in the presence of magnetic field. For the doping range of $x > 0.5$, the compound is an antiferromagnetic insulator with the ordering of doped charge carriers [8]. The half doped ($x = 0.5$) compound belonging to the system LCMO illustrates a complex mixture of low temperature ferromagnetic (FM) and antiferromagnetic (AFM)/charge ordered (CO) phases.[9-10]. This half doped compound at the phase boundary exhibits many extra ordinary properties and has been an interest of recent study [11-12]. Multifunctional magnetic nanoparticles have been synthesized and proved to be of valuable use especially in biomedical applications [12-14]. In this communiqué we investigated the synthesis of cubic $La_{0.5}Ca_{0.5}MnO_3$ by the substitution of divalent Ca form La in the parent compound $LaMnO_3$ and systematically investigated the related phenomenon by performing structural, electrical and magnetic analyses.

2. Experimental Details

Polycrystalline bulk samples of chemical composition $La_{0.5}Ca_{0.5}MnO_3$ were prepared by solid state reaction method using high purity (> 99.9%) precursors of La_2O_3, Mn_2O_3 and $CaCO_3$ taken in the stiochiometry ratio. Mixed powders were

Tele: +91-9419031528

E-mail addresses: ksbhat.phy@gmail.com

© 2013 Elixir All rights reserved

preheated at 1000^0C for 12 hours and calcinated again at 1200^0C for 12 hours. The homogenous powder was reground and pelletized into pellets of 10 mm in diameter by the application of 5 kN force. The resultant pellets were sintered at 1250^0C for 24 hours at a heating rate of 4^0Cmin^{-1} and then cooled to room temperature at a cooling rate of 3^0Cmin^{-1} in a tubular furnace.

The structure of the sample was analyzed by X-ray diffraction (XRD) using Bruker D8 Advance diffractometer (Cu-Kα radiation) at room temperature in the 2θ range of 20-80°. Raman study of the compound $La_{0.5}Ca_{0.5}MnO_3$ was carried out and the spectra was collected in back scattering geometry using an Ar excitation source having a wavelength of 488nm coupled with a Labram-HR800 micro Raman spectrometer equipped with a 50X objective, appropriate notch filter and a Peltier cooled charge-coupled device detector. No melting or phase transition was observed in the sample at excitation Laser power of 10 mW. For electrical resistivity measurement, four probe technique was carried out in the 5K - 300K temperature range at a step size of 1 deg./min.. For this, pellets were cut into rectangular bars of 8mm x 6mm. While the magnetic measurements were carried out using a QUANTUM DESIGN PPMS- VSM magnetometer with sensitivity upto 10^5 emu/g. The temperature dependent magnetization was carried out from 5K to 300K at a field of 500 Oe both in Field cooled (FC) as well as in Zero field cooled (ZFC) condition.

3. Results and discussions

3.1 XRD Analysis

The structure of $La_{0.5}Ca_{0.5}MnO_3$ was investigated by Rietveld treatment of the X-Ray diffraction (XRD) profiles recorded with a high- resolution diffractometer. The refined parameters include cell dimensions, 2θ zero point, half width and background parameters. Fig.1 shows XRD patterns of $La_{0.5}Ca_{0.5}MnO_3$ along with the fitted curves and the difference line, which clearly indicates that the XRD patterns are well fitted with orthorhombic structure, space group *Pnma*. The observed crystal structure as well as lattice parameters were in good agreement with results obtained earlier by Mahendiran et al. [16] where they found that the parent compound $LaMnO_3$ changes structure orthorhombic to cubic with 50% Ca doping.

Fig.1. XRD pattern of $La_{0.5}Ca_{0.5}MnO_3$ The structure of $La_{0.5}Ca_{0.5}MnO_3$ was investigated by Rietveld treatment of the X-Ray diffraction (XRD) profiles.

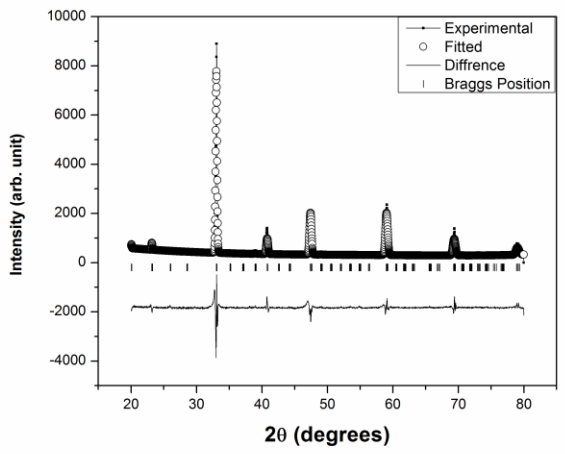

The cations La and Ca have almost similar size (see table I) and are randomly substituted on A site. The size of the ions determines the extent of distortion in the compound. If the size of A site cation $r_A < a/\sqrt{2}-r_o$ (here 'a' is the cubic lattice parameter and r_o is the radius of oxygen ion), the distortion will be most probably due to rigid tilts of oxygen octahedron. Whereas on contrarily if $r_B < a/2-r_o$ (r_B is the radius of B site cation) the distortion is most likely due to movement of B site cation within the oxygen octahedron. With these parameters and ionic sizes (from Table I) into consideration it is found that the system in present study follows the former ($r_A < a/\sqrt{2}-r_o$) relation between its contributing ions. This is suggestive of the fact that system will most probably distort by rotation of oxygen octahedral and this is what is observed at room temperature.

Table I. Ionic radii of constituent elements of $La_{0.5}Ca_{0.5}MnO_3$ (taken from [15]).

Ions and the formal valency	Coordination	Radius (Å)
La^{3+}	12	1.50
Ca^{2+}	12	1.48
Mn^{3+}	6	0.72
Mn^{4+}	6	0.67
O^{2-}	2	1.21

3.2 Raman study

Raman signature of perovskite structure can be attributed to be made of the two interpenetrated lattices: the covalent entities constituting the structure (BO6 octahedron sharing common oxygen ions) and the second one, made of highly Columbic ions that contribute to the translation oscillation modes which couple themselves with other vibrational modes of the neighboring entities: translations and rotations/Vibration of iono-covalent BO_6 entity leading to the wave number shifts. The Raman spectra at room temperature (300 K) of $La_{0.5}Ca_{0.5}MnO_3$ is shown in Fig.2. Raman peaks were observed at their finger point positions and following irreducible representations at the Brillouin zone center are presented by the group theory and are consistent with the literature [17].

$7A_g + 2B_{1g} + 7B_{2g} + 5B_{3g}$.

Taking MnO_6 into consideration, the above stated Raman modes can be classified in the following way. Primarily the Raman modes are classified into twelve internal and nine external modes. Out of twelve internal modes five are of stretching type [$A_g(1)$, $A_g(2)$, $B_{3g}(2)$, $B_{2g}(1)$, and 6 $B_{2g}(2)$] while the remaining seven internal modes are of bending type ($A_g(3)$, $A_g(4)$, $A_g(7)$, $B_{1g}(2)$, $B_{3g}(1)$, $B_{2g}(3)$, and $B_{2g}(7)$]. From the external modes six are of translational type [$A_g(5)$, $A_g(6)$, $B_{3g}(4)$, $B_{3g}(5)$, $B_{2g}(5)$, and $B_{2g}(6)$] and three are of rotational type [$B1g(1)$, $B3g(3)$, and $B2g(4)$]. On account of their high frequency, the Raman lines between 450 and 650 cm^{-1} correspond to internal modes [17-19]. The observed modes and the irreducible representations were consistent with the results of Abrashev et al. [20] for the composition $La_{0.5}Ca_{0.5}MnO_3$.

3.3 Electrical Resistivity

The electrical resistivity (ρ) was measured for selected compound within the temperature range of 5-300 K and the results are shown in fig.3. It is obvious from the graph that the ρ first increases as T decreases, exhibits a peak at T = Tp (Tp is the temperature corresponding to the resistivity peak) which is around 150 K in the present compound and then decreases as *T* is further reduced below *Tc* (Tc is the ferromagnetic curie temperature). For *T* > *Tc* , the resistivity shows activated transport as in an insulator. Activation energy (E_a) was calculated from the slope of the curve log ρ vs 1000/T (K^{-1}) using relation $\rho = \rho_0 e^{-Ea/kT}$ and was found to be equal to 0.13 eV. Here ρ_0 is the conductivity at infinite temperature and k is the Boltzmann's constant and *Ea* is the activation energy.

Fig.2. Raman spectra of $La_{0.5}Ca_{0.5}MnO_3$, the spectra was collected in back scattering geometry using an Ar excitation source

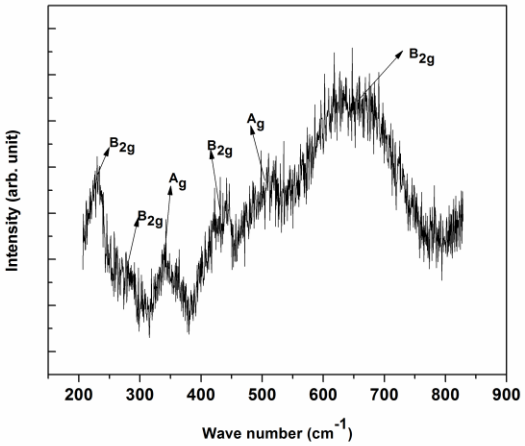

The resistivity at the highest temperature measured (ρ_{300K}) is less than that at 5 K ($\rho_{5\ K}$). Although for T< Tp, the material shows a metal-like variation of resistivity with temperature ($d\rho/dT > 0$). The reported results were in good agreement with the literature [16]. It is clear from the fig.3 that a metal like behavior is observed for temperature T < Tp. The resistivity at lowest measured temperature is ~ 40 Ωcm which is very high compared to the typical Mott resistivity (ρ_{Mott}). One of the possible reasons for this high resistivity may be the grain boundaries [21].

Fig.3. Temperature variation of resistivity of polycrystalline pellets of $La_{0.5}Ca_{0.5}MnO_3$. The resistivity at the highest temperature measured (ρ_{300K}) is less than that at 5 K ($\rho_{5\ K}$)

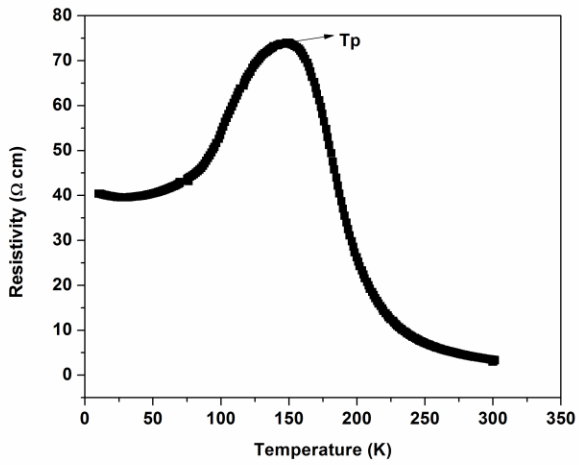

3.3 Magnetic measurements

The zero-field-cooled (ZFC) and field-cooled (FC) magnetization as a function of temperature at 500 Oe field are shown in fig. 4, while as the magnetization vs field (MH) curves at 5 K and 300 K are shown in fig. 5. The sample shows irreversible behavior with closed loops of ZFC and FC curves. The large difference between *M*FC and *M*ZFC at low temperatures suggests an inhomogeneous mixture of a ferromagnetic and antiferromagnetic rather than a distinct ferromagnetic or antiferromagnetic long range order. Mixed valent manganites are noted for their unusual magnetic, electronic and structural phase transitions. The compound $La_{0.5}Ca_{0.5}MnO_3$ shows coexistence of two totally dissimilar ground states i,e ferromagnetic-metallic and antiferromagnetic-charge ordered which is also consistent with the earlier reports [22-23].

Table II gives the values of various calculated parameters for the compound $La_{0.5}Ca_{0.5}MnO_3$. A qualitative picture of the behavior displayed by the mixed valent manganite $La_{0.5}Ca_{0.5}MnO_3$ can be attributed to the concept of Zener double exchange [24]. Actually it revolves around the changing valency of Mn from $Mn^{4+} \leftrightarrow Mn^{3+}$ i,e there is hopping of a 3d hole from Mn^{4+} (d^3, $T_{2g}(3)$, S=3/2), to Mn^{3+} (d^4, $T_{2g}(3)$, e_g (1), S=2), via the intervening ligand oxygen. Electrons are thought to hop between neighboring Mn ions via the intervening oxygen atom. During hopping spin of electrons will be preserved provided some scattering doesn't take place during transfer of electrons. The ferromagnetic alignment is energetically favourable as Hund's rule coupling makes it favourable for the spin of core electrons to align with the spin of the itinerant electrons.

Table II. gives the values of various calculated parameters for the compound $La_{0.5}Ca_{0.5}MnO_3$

Compound	Crystal Structure	Lattice Parameter (Å) a	b	c	Tc (K)	Tp (K)	Ea (eV)
$La_{0.5}Ca_{0.5}MnO_3$	Orthorhombic (*pnma*)	5.543	7.721	5.641	250	150	0.13

Fig.4. Magnetization versus temperature plot for $La_{0.5}Ca_{0.5}MnO_3$ sample in the presence of 500 Oe magnetic field. It is seen that that the compound shows both a paramagnetic to ferromagnetic transition and an antiferromagnetic transition at around 170 K.

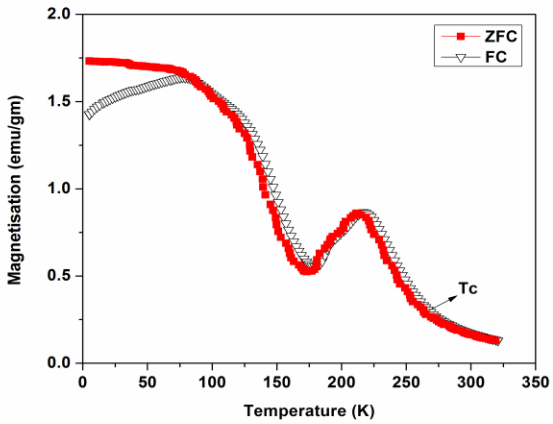

Fig.5. M vs H curves at 5 K and 300 K $La_{0.5}Ca_{0.5}MnO_3$. It is seen from the figures that there is clear magnetic transition from 5 K to 300 K.

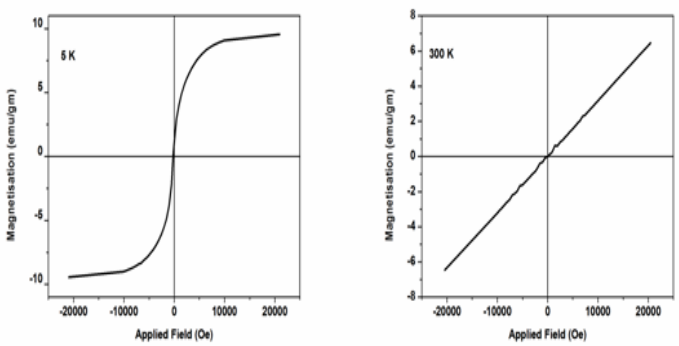

This hopping of electrons between Mn ions is also responsible for conductivity in the compound. The oxygen between Mn ions is regarded as having a passive role in the

conduction process. The core spins of every Mn ion is aligned parallel in ferromagnetic phase so has the best conductivity whereas antiferromagnetic phase has the antiparallel arrangement of core spins and has the least conductivity, while as the conductivity of paramagnetic phase is intermediate. Based on this zener double exchange a paramagnetic to ferromagnetic transition occurs in the compound. From fig. 4 it is clear that the compound shows both a paramagnetic to ferromagnetic transition at around 250 K and then an antiferromagnetic transition at around 170 K. The large hysteresis is reported in literature for these compounds [25-26]. This observed hysteresis proves to be an indication that charge ordering is a nucleation and growth process. The compound $La_{0.5}Ca_{0.5}MnO_3$ illustrates a complex mixture of low temperature ferromagnetic and antiferromagnetic /charge ordered phases. At temperatures well below the Neel temperature, the magnetization for the compound is still higher possibly due to two reasons: spin canting [27-28] or an inhomogeneous mixture of ferromagnetic and antiferromagnetic regions within the compound.

4. Conclusion

Polycrystalline bulk compounds of $La_{0.5}Ca_{0.5}MnO_3$ were synthesized by solid state reaction technique. Rietveld treatment of the XRD profiles clearly indicated that the XRD patterns are well fitted with cubic structure, space group *Pnma* and lattice parameter of 7.645 Å. Raman peaks were observed at their finger point positions. The results of transport measurements clearly show that $T > Tc$, the resistivity shows activated transport as in an insulator. From the magnetic measurements it is obvious that the compound shows both a paramagnetic to ferromagnetic transition at around 250 K and then an antiferromagnetic transition at around 170 K. A complex mixture of low temperature ferromagnetic and antiferromagnetic /charge ordered phase was seen in the compound. The qualitative picture of the behavior displayed by the mixed valent manganite $La_{0.5}Ca_{0.5}MnO_3$ was attributed to the concept of Zener double exchange.

Acknowledgements

Authors (K.S and M.I) thank Dr. Alok Banerjee IUC, CSR Indore for the magnetic measurements, Director IUAC, New Delhi for necessary experimental facilities. Authors would also like to thank Director NIT Srinagar for encouragement provided during work.

References

1. A. P. Ramirez, J. Phys.: Condens. Matter , 9, **1997**, 8171.
2 Radheshyam Rai, Indrani Coondoo, M.A. Valente,. ; Andrei L. Kholkin Adv. Mat. Lett. 4(5), **2013**, 354-358.
3. MB Salamon; M. Jaime, Rev. Mod. Phys. 73, **2001**, , 583.
4. EO Wollan, Koehler, WC. Phys. Rev. 100, **1995**, 545.
5. P. Schlottmann,. Phys. Rev. B 77, **2008**, , 104446.
6. Goodenough, J. Phys. Rev. 100, **1955**, 564.
7. R.Von Helmolt,; J. Wecker, Holzapfel, B.; Schultz, L.; Samwer, K. Phys. Rev. Lett. 71**, 1993**, 2331.
8. P. Schiffer, A.P Ramirez, W. Bao, SW Cheong, Phys. Rev. Lett. 75, **1995**, 3336.
9. S. Mori, C.H Chen, S. Cheong, Phys. Rev. Lett. 81, **1998**, 3972-3975.
10. Y. Tomioka, A. Asamitsu, Y. Moritomo, H. Kuwahara, Y. Tokura, Phys. Rev. Lett. 74, **1995**, 5108.
11. P.G Radaelli, D.E Cox, M. Marezio, S.W Cheong, P.E Schiffer, A.P Ramirez, Phys. Rev. Lett. 75, **1995**, 4488.
12. M. Singh, M. Kumar, Štěpánek, F.PUlbrich, P. Svoboda, E. Santava, M. L Singla, Adv. Mat. Lett.2, **2011**, 409-414.
13. P. K Sharma, R.K Dutta, A.C Pandey, Adv. Mat. Lett. 2, **2011**, 246-263.
14. H. Zhao, Z. Zhang, Z. Zhao, R. Yu, Y. Wan, M. Lan, M Adv. Mat. Lett. 2, **2011**, 172-175.
15. R.D Shannon *Acta*. *Cryst*. 32, **1976**, A 751–767.
16. R. Mahendiran, S.K Tiwary, A.K Raychaudhuri, T.V Ramakrishnan, Phys. Rev. B. 53, **1996**, 6 1.
17. S. Yoon, M. Ru¨bhausen, S.L Cooper, K.H Kim, S.W Cheong, Phys. Rev. Lett. 85 **2000**, 3297.
18. K. Yamamoto, T. Kimura, T. Ishikawa, T. Katsufuji, and Y. Tokura, Phys. Rev. B. 61, **2000**, 14706.
19. D.N Argiriou, H.N Bordallo, B.J Campbell, A.K Cheetham, D.E Cox, J.S Gardner, K. Hanif, A. Dos Santos, G.F Strouse, Phys. Rev. B.61, **2000**, 15269.
20. M.V Abrashev, J. Backstrom, L. Borjesson, Phys. Rev. B. 64, **2001**, 144429.
21.P. P. Edwards, M. J. Sienko, Phys. Rev. B.**1978**, **17**, 2575.
22. A. Moreo, S. Yunoki, E. Dagotto, Phase separation scenario for manganese oxides and related materials. *Science* 283, **1999** 2034–2040.
23. N.D Mathur, P.B Littlewood, The self-organised phases of manganites. *Sol*. *Stat*. *Comm*. 119, **2001**, 271-280.
24. C. Zener, Phys. Rev. 82, **1951**, 403.
25. M. Uehara, S. Mori, C.H Chen, S.W Cheong Percolative phase separartion underlies colossal magnetoresistance in mixed valent manganites. *Nature* 399, **1999**, 560–563.
26. P. Levy, *et al*. Controlled phase separation in La0.5Ca0.5MnO3. *Phys. Rev*.
B .62, **2000**, 6437–6441.
27. P.G Radaelli, D.E Cox, L. Capogna, S.W Cheong, M. Marezio, Wigner-crystal and bi-stripe models for the magnetic and crystallographic superstructures of La0.333Ca0.667MnO3. *Phys. Rev. B*. 59, ***1999,*** 14440–14450.
28. M. Roy, J. F Mitchell, A.P Ramirez, P. Schiffer Doping-induced transition from double exchange to charge order in La1-*x*Ca*x*MnO3 near $x = 0.5$ *Phys. Rev. B* **.** 58, **1998**, 5185–5188.